CELL BIOCHEMISTRY & FUNCTION

CELL BIOCHEMISTRY AND FUNCTION
Cell Biochem Funct 2016; **34**: 299–309.
Published online 3 May 2016 in Wiley Online Library
(wileyonlinelibrary.com) **DOI**: 10.1002/cbf.3190

Differential expression of long non-coding RNAs in hyperoxia-induced bronchopulmonary dysplasia

Tian-Ping Bao[1†], Rong Wu[2†], Huai-Ping Cheng[1], Xian-Wei Cui[3]* and Zhao-Fang Tian[1]*

[1]*Department of Neonatology, Huai'an First People's Hospital, Nanjing Medical University, Huai'an, Jiangsu, China*
[2]*Neonatal Medical Centre, Huai'an Maternity and Child Healthcare Hospital, Huai'an, Jiangsu, China*
[3]*Nanjing Maternity and Child Health Care Institute, Nanjing Maternity and Child Health Care Hospital, Nanjing Medical University, Nanjing, Jiangsu, China*

Bronchopulmonary dysplasia (BPD) is a common complication of premature birth that seriously affects the survival rate and quality of life among preterm neonates. Long non-coding RNAs (lncRNAs) have been implicated in many human diseases. However, the role of lncRNAs in the pathogenesis of BPD remains poorly understood. Here, we exposed neonatal C57BL/6J mice to 95% concentrations of ambient oxygen and established a mouse lung injury model that mimicked human BPD. Next, we compared lncRNA and messenger RNA (mRNA) expression profiles between BPD and normal lung tissues using a high-throughput mouse lncRNA + mRNA array system. Compared with the control group, 882 lncRNAs were upregulated, and 887 lncRNAs were downregulated in BPD lung tissues. We validated some candidate BPD-associated lncRNAs by real-time quantitative reverse-transcription polymerase chain reaction analysis in eight pairs of BPD and normal lung tissues. Gene ontology, pathway and bioinformatics analyses revealed that a downregulated lncRNA, namely AK033210, associated with tenascin C may be involved in the pathogenesis of BPD. To the best of our knowledge, our study is the first to reveal differential lncRNA expression in BPD, which provides a foundation for further understanding of the molecular mechanism of BPD development.

KEY WORDS—long non-coding RNA; bronchopulmonary dysplasia; hyperoxia; microarray analysis

INTRODUCTION

Bronchopulmonary dysplasia (BPD) was first described in 1967 by Northway *et al*. to develop from prolonged mechanical ventilation of the surfactant-deficient lung with high pressures and concentrations of inspired oxygen.[1] BPD was initially defined as postnatal 28 days of requiring oxygen with representative radiographic changes and occurred in relatively large premature infants characterized by intense airway inflammation and lung fibrosis. With the advances in perinatal care, including antenatal steroids, routine surfactant replacement and the introduction of optimized ventilation strategies, more premature infants survive at lower gestational age (22–28 weeks) and lower birth weight (501–1500 g).[2] Because of these improvements in neonatal intensive care, the severe form of "classic BPD" has been much less common and replaced by a milder clinical form, which often occurs in very-low-birth-weight neonates and is characterized primarily by the arrest of alveolar and vascular development.[3] Pathologically, alveolar numbers are reduced, while the diameters of alveoli are larger. Infants who have smaller gestation age and lower body weight are at a greater risk of developing BPD. Most of these infants are born without the need for oxygen-inhaling devices but then gradually come to depend on oxygen. Complications accompanied by survivors include airway hyperresponsiveness diseases, recurrent lower respiratory tract infections, feeding intolerance and growth retardation. Therefore, BPD has become one of the most intractable problems in neonatal intensive care unit and seriously affects the survival rate and quality of life of premature infants.

Immaturity, perinatal infection and inflammation, oxidative stress and fibrosis play crucial roles in BPD progression.[4,5] However, the aetiology of BPD is multifactorial, and genetic predisposition plays an important role in BPD pathogenesis.[6] Long non-coding RNAs (lncRNAs) play crucial roles in regulating gene expression during lung development. Szafranski *et al*. found that a lack of a specific lncRNA could result in fatal pulmonary and vascular dysplasia.[7] In addition, Sauvageau *et al*. confirmed that knockout of a specific rat lncRNA led to abnormal lung growth and development.[8]

*Correspondence to: Zhao-Fang Tian, Department of Neonatology, Huai'an First People's Hospital, Nanjing Medical University, 6 Beijing Road West, Huai'an, Jiangsu 223300, China.
E-mail: tianzhaofan@163.com; Xian-Wei Cui, Nanjing Maternity and Child Health Care Institute, Nanjing Maternity and Child Health Care Hospital, Nanjing Medical University, Nanjing, 210029, China.
E-mail: cuixianwei198615@126.com
†These authors contributed equally to this work as first authors.

Received 24 January 2016
Revised 11 April 2016
Accepted 12 April 2016

Recent progress in high-resolution microarray analysis and genome-wide sequencing technology makes it possible to gain insight into molecular mechanisms of diseases. lncRNAs, defined as transcripts of greater than 200 nucleotides without protein-coding function, have generated considerable interest in the past decade.[9] Large numbers of lncRNAs have been identified, and they are implicated in human diseases by regulating oxidative stress, inflammation, apoptosis, cell growth and viability.[10–13] However, the expression profile and biological function of lncRNAs in BPD are currently unknown.

In this study, we successfully established a neonatal murine model of hyperoxia-induced BPD. We compared the expression profiles of lncRNAs and messenger RNAs (mRNAs) in the lung tissues of BPD and normal control groups and then validated several differentially expressed lncRNAs by quantitative real-time polymerase chain reaction (PCR) in eight pairs of tissue samples. Our results suggest that abnormal lncRNA expression patterns may play an important role in BPD development.

MATERIALS AND METHODS

Animal model

Pregnant C57BL/6J mice with approximate gestation age were purchased from the Experimental Animal Center of Nanjing Medical University. Twenty neonatal mice born within 3 h were randomly assigned to room air and hyperoxia ($FiO_2 \geq 95\%$ for 7 days). Adult and neonatal C57BL/6J mice were housed in pathogen-free rooms on a 12:12-h light–dark cycle, and we followed our institutional guidelines for animal care. Hyperoxia exposure was accomplished in an 80 cm × 50 cm × 60 cm Plexiglas chamber, which was continuously aerated at a rate of $5\,L{\cdot}min^{-1}$. Oxygen concentration was monitored with an oxygen meter. Nursing dams were alternated between the air and hyperoxia litters every 24 h to prevent oxygen toxicity in the dams.

Lung samples and morphological analysis

Neonatal mice were anaesthetized by intraperitoneal injection of 4% chloral hydrate $0{\cdot}1\,ml{\cdot}g^{-1}$ after 7 days of exposure. We opened the chest cavity, punctured at the strongest heart throb, and inflated the heart with phosphate-buffered saline until the left and right lungs turned white. The left and right upper lungs were snap-frozen in liquid nitrogen immediately and stored at −80 °C. The rest of the lungs were soaked in 4% paraformaldehyde solution and then fixed overnight at 4 °C; the tissue was dehydrated and paraffin embedded, cut into 5-μm sections, stained with haematoxylin and eosin and examined with light microscopy. Radial alveolar counts were calculated as described previously[14]: A perpendicular line was drawn from the centre of the respiratory bronchiole to the edge of the acinus, and the septa intersected by that line were counted.

RNA extraction and quality control

Total RNA was extracted from frozen lung samples with a TRIzol reagent (Invitrogen, Carlsbad, CA, USA) according to the manufacturer's protocol and was quantified using a NanoDrop ND-1000 spectrophotometer (Agilent, Santa Clara, CA, USA) to measure the absorbance ratios of OD260/OD280. All ratios were between 1.8 and 2.0, and RNA integrity was assessed via denaturing agarose gel electrophoresis. Genomic DNA was removed from RNA samples with TaKaRa Transcript RNA Clean-up Kit.

Microarray

Three pairs of BPD and control lung tissues were used for lncRNA microarray analysis. Arraystar Mouse lncRNA Microarray V3.0 was used to profile mouse lncRNAs and protein-coding genes (Kangcheng, Shanghai, China). A total of 35 923 mouse lncRNAs were identified from authoritative databases, such as "RefSeq_NR", "UCSC_knowngene", "Ensemble", "ultra-conserved region (UCR)", "lincRNA" and other previously identified lncRNAs. Probes for housekeeping genes and negative controls were printed multiple times to ensure hybridization quality. Sample preparation and microarray hybridization were performed based on the manufacturer's standard protocols with minor modifications. Differentially expressed lncRNAs were identified by volcano plot filtering, and upregulated or downregulated lncRNAs were screened using the threshold of fold change ≥2.0 ($p < 0.05$).

Quantitative real-time PCR

Total RNA was extracted from frozen lung tissues using a TRIzol reagent (Invitrogen). One microgramme of total RNA from each sample was reverse transcribed to complementary DNA (cDNA) using a random hexamer primer with a Thermo Scientific RevertAid First Strand cDNA Synthesis Kit (Thermo Scientific, Wilmington, DE, USA). Fifteen distinct lncRNAs were validated in eight pairs of BPD and control lung tissue samples by quantitative PCR (qPCR) performed in triplicate using SYBR green I dye (Takara, Dalian, China) on Applied Biosystems ViiA™ 7 DX (Life Technologies, USA). All primers used in the study were shown in Table 1. PCR conditions were as follows: an initial denaturation step at 95 °C for 30 s, followed by 40 cycles of 95 °C for 5 s and 60 °C for 35 s. The expression levels were normalized to glyceraldehyde 3-phosphate dehydrogenase as internal control and calculated using the $2^{-\Delta\Delta CT}$ method.[15]

GO and pathway analyses

Pathway and gene ontology (GO) analyses were applied to determine the role of genes in biological pathways or GO terms. The GO is a controlled vocabulary composed of >38 000 precise defined phrases called GO terms that describe the molecular actions of gene products, the biological processes in which those actions occur and the cellular locations where they are present (http://www.geneontology.org).

Table 1. Polymerase chain reaction primers used in this study

Gene	Primer	Sequence (5′–3′)
Primers for lncRNAs		
Gm11485	Forward	ACAAGCCAACGAAGCAGAGA
	Reverse	TCTCGATCAGCATCACAGGC
Gm16263	Forward	ACTGAAACTCTCGGCACTGG
	Reverse	GCCCTGAGTTTGGTTTGCAG
AK028951	Forward	TCCTGGGAGGAATGGACACT
	Reverse	TCCAGCTGAGTCATGTCACG
AK158295	Forward	GCATGGACATAGCCCCTACC
	Reverse	CTTGTAAGGCCCACTCAGGG
Kif2c	Forward	CTTCACGCACGCCTGTTTC
	Reverse	CTCCTTCGATCCATTCCACCG
4930546k05Rik	Forward	CCAGACTGAGTGGGGTGAAC
	Reverse	GGTCTGGGCACTGCCATTAT
Gm12192	Forward	GAAGGCCATGCAGTCTCTCA
	Reverse	GGCAGGCACAATCTCCAGAA
AK144143	Forward	TTCTCCTTTAGCCTTCACCATTCTT
	Reverse	TTCCTACCTACCCTATCCAGCAC
Gm20475	Forward	TTGAGGGCGAAAGTTCTGTAGGA
	Reverse	CACAGCCTCGGAATCTTTACTGATA
AK033210	Forward	CCTGGAGTTGGTTTCCCCTC
	Reverse	ACCAGCCAAATCAGAGAGCC
Smgc	Forward	TGGAGCTGGCTTCTATACTTCC
	Reverse	TCCCAGGTAACCTAACAGACTC
Sult1d1	Forward	TCTTCAGGAGGGAGTTAGTGG
	Reverse	GGCCGGGCTTCAAATGACT
4930539M17Rik	Forward	GGCAAGCAGCCTACCTAACA
	Reverse	CCGGCTAGACACCCATGTTT
AK132613	Forward	AATGTACACCACGTTGGGCT
	Reverse	GTGGGCAGAGGTTCCTTTCA
AK076683	Forward	GATCCGTCTGTTTCAGCCCA
	Reverse	GAGCCATTTCAGTGTCCCCA
Primer for associated gene		
TNC	Forward	TTTGCCCTCACTCCCGAAG
	Reverse	AGGGTCATGTTTAGCCCACTC
TGF-β	Forward	GGTGTGAACTGTCACCGATCA
	Reverse	GTTTAGGATGTGAACCTCCCTTG
IGF-1	Forward	GGGACTCAAGTATTCCTTTCCTG
	Reverse	GCACCTGGACAGCTATATTGAC
VEGF-α	Forward	AAAGGGAAAGGGTCAAAAACGAA
	Reverse	AGGAACATTTACACGTCTGCGG
GAPDH	Forward	AGGCCGGTGCTGAGTATGTC
	Reverse	TGCCTGCTTCACCACCTTCT

GAPDH, glyceraldehyde 3-phosphate dehydrogenase; IGF-1, insulin-like growth factor 1; lncRNA, long non-coding RNA; TGF-β, transforming growth factor β; TNC, tenascin C; VEGF-α, vascular endothelial growth factor α.

Pathway analysis is a functional analysis mapping genes to the Kyoto Encyclopaedia of Genes and Genomes (KEGG) pathways. GO term enrichment and KEGG pathway analyses were performed based on DAVID 6.7 (http://david.abcc.ncifcrf.gov/home.jsp) ($p < 0.01$).

Statistical analysis

All results were presented as means ± standard deviations. To screen differentially expressed lncRNAs, we followed the criteria of threshold values of ≥2-fold and ≤ -2-fold changes and a Benjamini–Hochberg corrected p-value of 0.05.

RESULTS

Animal survival

Two mice of the hyperoxia-exposed group died from the initial hyperoxia exposure by the end of the experiment, but no mice died in the control group. To maintain the size of the groups for the same nursing care, we rejected an equal number of control mice randomly immediately after the death of hyperoxia mice. The surviving hyperoxia-exposed mice had lower body weight and less activity.

Stereological analysis and biomarkers of mouse BPD model

Prolonged hyperoxia caused pathological alterations in both lung morphology and structure (Figure 1A and B). Exposure of neonatal mice to 95% O_2 reduced radial alveolar count by 32% (Figure 1C). Additionally, we detected changes in the expression levels of several well-known BPD biomarkers (Figure 1D). As reported previously, transforming growth factor β (TGF-β) drives pulmonary fibrosis and inhibits lung development[16]; in this study, mRNA expression of TGF-β increased 3.2-fold. The mRNA level of insulin-like growth factor 1, a profibrogenic mediator involved in stimulating collagen synthesis,[17] increased by 4-fold. In contrast, the mRNA level of vascular endothelial growth factor α, which can promote alveolar epithelial proliferation and regulate angiogenesis,[18] decreased by 60%. These pathological pulmonary changes together with BPD biomarker changes were similar to human BPD.

Overview of lncRNA profiles

To explore the potential biological function of lncRNAs in BPD, we compared lncRNA and mRNA expression profiles between BPD and normal groups using microarray analysis. In total, 35 923 lncRNAs and 24 881 coding transcripts were detected, which were collected from authoritative databases such as RefSeq, UCSC_known-gene, Ensemble and related literature. The scatter plot was used to evaluate lncRNA expression variation between the two groups (Figure 2A). Hierarchical clustering showed lncRNA expression patterns of the two groups (Figure 2B). A total of 887 lncRNAs were downregulated more than twofold in the BPD group as compared with the normal group, whereas 882 lncRNAs were upregulated more than twofold ($p < 0.05$). Furthermore, 60 upregulated lncRNAs and 13 downregulated lncRNAs were identified by the fold change ≥ 7 ($p < 0.01$) as shown in Table 2, and these lncRNAs were likely to be involved in the development of BPD.

Overview of mRNA profiles

A total of 24 881 coding transcripts were detected in the lung samples, of which 1397 mRNAs were differentially expressed between BPD and normal groups, including 467 mRNAs upregulated and 930 mRNAs downregulated (fold change ≥ 2, $p < 0.05$). Notably, 28 mRNAs were identified to be upregulated while 40 mRNAs were downregulated

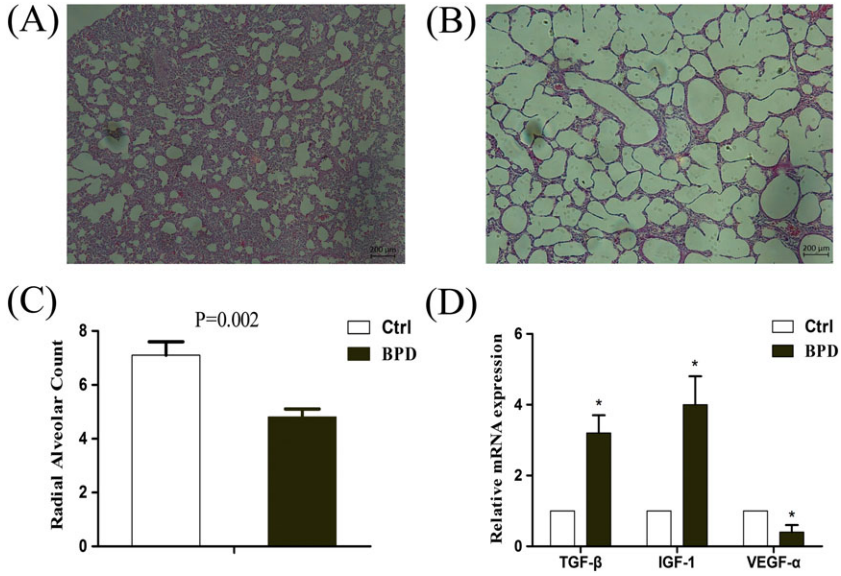

Figure 1. Effects of hyperoxia on neonatal mouse lung. Inflated lungs were paraffin embedded, and 5-μm tissue sections were stained with haematoxylin and eosin. All pictures were taken at 100× magnification. Calibration bar is 200 μm. (A) Exposure to room air at postnatal day 7 (control group). (B) Exposure to hyperoxia at postnatal day 7 (BPD group). (C) Under the microscope magnifying 100×, five sections of each sample in five random sights were selected for radial alveolar count in eight pairs of BPD and control lung tissue samples. The radial alveolar count is significantly different at postnatal day 7 ($p = 0{\cdot}002$). The bars indicate standard deviations.(D) Relative mRNA expression of several biomarkers of BPD by real-time polymerase chain reaction comparing mouse lung exposed to room air with that exposed to hyperoxia ($*p < 0{\cdot}05$) in eight pairs of BPD and control lung tissue samples. BPD, bronchopulmonary dysplasia; Ctrl, control; IGF-1, insulin-like growth factor 1; TGF-β, transforming growth factor β; VEGF-α, vascular endothelial growth factor α

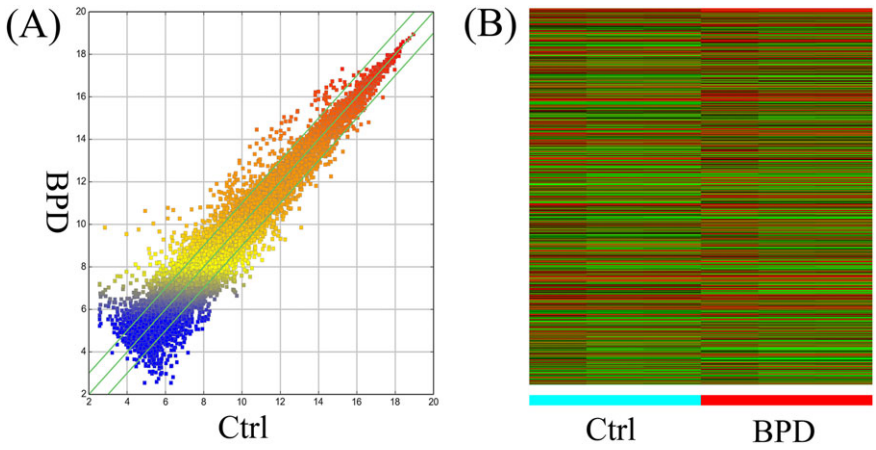

Figure 2. Profile of the microarray data. (A) The scatter plot is used for evaluating the lncRNA expression variation between the control (Ctrl) and bronchopulmonary dysplasia (BPD) groups. Long non-coding RNAs (lncRNAs) above the top green line and below the bottom green line showed more than threefold expression change between the two compared groups. (B) A total of six arrays were performed at the same time. Hierarchical clustering shows a remarkable lncRNA expression profile change between the two compared groups

by more than sevenfold ($p < 0.01$) (a list of markedly distinct mRNAs shown in Table 3).

Expression signatures of dysregulated lncRNAs

We described some signatures of dysregulated lncRNAs in terms of chromosome distribution, length distribution, classification and sources. Chromosome distribution reflects the numbers of dysregulated lncRNAs at various chromosome locations (Figure 3A). The lengths of these lncRNAs fell mainly between 200 and 3600 bp (Figure 3B). Among these dysregulated lncRNAs, there were 591 sense overlaps, 386 antisense overlaps and 101 bidirectional and 691 intergenic RNAs (Figure 3C). Figure 3D showed the percentage of dysregulated lncRNAs identified from different databases.

Table 2. Long non-coding RNAs implicated in bronchopulmonary dysplasia

Gene symbol	Source	RNA length	Chromosome	Log2 (O_2-treated/room air)
Mup-ps19	Ensembl	519	chr4	−13·293
Ahsg	RefSeq	1439	chr16	−11·888
Gm19990	RefSeq	1221	chr12	−9·413
Nlrp5-ps	RefSeq	3919	chr7	−9·230
C130080G10Rik	RefSeq	1909	chr2	−8·296
AK134233	GenBank	2190	chr8	−7·827
Nusap1	Ensembl	557	chr2	−7·733
2810442I21Rik	Ensembl	787	chr11	−7·658
AK156967	UCSC_kg	416	chr14	−7·653
XLOC_025643	Alexander *et al*. 2013	2573	chr9	−7·424
Gm13176	Ensembl	477	chr2	−7·352
AK031221	UCSC_kg	2760	chr7	−7·170
AK084660	GenBank	2386	chr10	−7·160
XLOC_000111	Alexander *et al*. 2013	2198	chr1	7·168
Serpina3e-ps	Ensembl	1228	chr12	7·168
AK141565	UCSC_kg	2203	chr3	7·175
Fah	Ensembl	658	chr7	7·270
humanlincRNA2050	lincRNA	458	chr11	7·302
AK140097	GenBank	2657	chr7	7·421
Alox5	Ensembl	3576	chr6	7·547
BC086315	UCSC_kg	3329	chr14	7·645
AK156090	GenBank	1497	chr15	7·663
Bai3	Ensembl	4569	chr1	7·671
2610017I09Rik	Ensembl	682	chr1	7·897
Pak7	Ensembl	2097	chr2	8·136
AK144783	GenBank	2788	chr6	8·185
Nwd1	Ensembl	4126	chr8	8·288
AK146794	GenBank	597	chr2	8·298
humanlincRNA1712	lincRNA	9743	chr13	8·414
Dlx6os1	Ensembl	4503	chr6	8·645
C130071C03Rik	Ensembl	3416	chr13	8·728
AK046285	GenBank	1478	chr7	8·778
Gm3892	Ensembl	1395	chr4	8·785
AK143973	GenBank	1852	chr16	8·871
Gm14204	RefSeq	1554	chr2	8·977
Gm6754	Ensembl	913	chrX	8·998
AK015661	GenBank	1241	chrX	9·035
4833428L15Rik	RefSeq	1259	chr9	9·155
AK039729	GenBank	1164	chr7	9·446
AK087397	GenBank	1324	chr11	9·505
Lrfn5	Ensembl	4009	chr12	9·529
AK132645	GenBank	1535	chr12	9·584
Npr1	Ensembl	949	chr3	9·642
AK051713	GenBank	3258	chr8	9·887
AK040275	GenBank	2988	chr4	9·970
AK076311	GenBank	2268	chr14	10·056
Gm10863	UCSC_kg	905	chr15	10·162
AK138478	GenBank	2739	chr16	10·348
Olfr990-ps1	Ensembl	896	chr2	10·468
Nupr1	Ensembl	2449	chr7	10·556
Rmst	Ensembl	2698	chr10	10·969
AK020757	GenBank	963	chr14	11·170
AK020832	GenBank	897	chr5	12·235
AK013470	GenBank	1544	chr19	12·889
AK008754	GenBank	1313	chr11	13·172
AK032235	GenBank	2727	chr6	13·517
AK005616	UCSC_kg	759	chr4	14·074
AK089129	GenBank	2233	chr6	14·884
Cryba1	Ensembl	1377	chr11	15·845
AK030618	GenBank	1611	chr3	15·849
AK005214	UCSC_kg	416	chr10	15·881
3110039M20Rik	RefSeq	870	chr12	15·892
D7Ertd715e	UCSC_kg	6765	chr7	16·117
Gm5859	UCSC_kg	1147	chr4_GL456350_random	16·772
H2-Bl	Ensembl	1072	chr17	16·775

(*Continues*)

Table 2. (Continued)

Gene symbol	Source	RNA length	Chromosome	Log2 (O_2-treated/room air)
AK015642	GenBank	1383	chr7	16·994
AK082001	GenBank	2228	chr6	17·842
Xist	Ensembl	626	chrX	17·917
Eda2r	Ensembl	779	chrX	19·357
BC056457	UCSC_kg	757	chr12	24·251
A930011O12Rik	Ensembl	3822	chr14	25·079
AK047207	GenBank	526	chr4_GL456350_random	25·255
C130071C03Rik	Ensembl	2427	chr13	25·571

Validation of dysregulated lncRNAs

We selected five upregulated lncRNAs and ten downregulated lncRNAs based on fold difference and nearby encoding genes to verify the microarray data. qPCR analysis showed that the expression of Smgc, Sult1d1, 4930539M17Rik, AK132613 and AK076683 increased, whereas the expression of Gm11485, Gm16263, AK028951, AK158295, kif2c, 4930546k05Rik, Gm12192, AK144143, Gm20475 and AK033210 decreased during hyperoxia-induced BPD (all $p < 0.05$; Figure 4). The results validated the microarray data.

GO and pathway analyses

Gene ontology analysis showed that among the upregulated mRNAs, 801 genes were involved in biological processes, 51 genes involved in cellular components and 116 genes involved in molecular functions. The top ten GO terms associated with neighbouring coding gene functions of upregulated lncRNAs were the following (Figure 5A): (1) GO 0048519, negative regulation of biological process; (2) GO 0051239, regulation of multicellular organismal process; (3) GO 0040011, locomotion; (4) GO 0050793, regulation of developmental process; (5) GO 0044699, single-organism process (growth and development for single organ or tissue); (6) GO 2000026, regulation of multicellular organismal development; (7) GO 0048518, positive regulation of biological process; (8) GO 0006950, response to stress; (9) GO 0048523, negative regulation of cellular process; and (10) GO 0030514, cell differentiation. Meanwhile, among the downregulated mRNAs, 819 genes were involved in biological processes, 126 genes involved in cellular components and 112 genes involved in molecular functions. The top ten GO terms associated with neighbouring coding gene function of downregulated lncRNAs were the following (Figure 5B): (1) GO 0007049, cell cycle; (2) GO 0051301, cell division; (3) GO 0000280, nuclear division; (4) GO 0006259, DNA metabolic process; (5) GO 0007067, mitotic nuclear division; (6) GO 0048285, organelle fission; (7) GO 1903047, mitotic cell cycle process; (8) GO 0022402, cell cycle process; (9) GO 0000278, mitotic cell cycle; and (10) GO 0006335, DNA replication-dependent nucleosome assembly.

Pathway analysis is a functional analysis technique that maps genes to KEGG pathways. The top ten pathways associated with neighbouring coding gene functions of upregulated lncRNAs were the following (Figure 5C): (1) p53 signalling pathway; (2) cytokine–cytokine receptor interaction; (3) prion diseases; (4) Chagas disease; (5) tumour necrosis factor signalling pathway; (6) vitamin digestion and absorption; (7) asthma; (8) chronic myeloid leukaemia; (9) *Staphylococcus aureus* infection; and (10) chemokine signalling pathway. The top ten pathways associated with coding gene functions of downregulated lncRNAs were the following (Figure 5D): (1) systemic lupus erythematosus; (2) alcoholism; (3) cell cycle; (4) DNA replication; (5) viral carcinogenesis; (6) complement and coagulation cascades; (7) mismatch repair; (8) oocyte meiosis; (9) pyrimidine metabolism; and (10) transcriptional dysregulation in cancer.

Bioinformatics analysis

We selected the dysregulated lncRNAs with higher expression fold changes and those that were positioned near coding genes involved in BPD. We found a downregulated lncRNA, AK033210, which was an intronic antisense lncRNA located near the tenascin C (TNC) gene. AK033210 was expressed at a lower level in BPD lung tissues than in normal lung tissues. Our microarray and qPCR analyses indicated that TNC mRNA expression was higher during the development of BPD than in controls (Figure 6).

DISCUSSION

Between 2003 and 2007, 68% of premature infants at 22–28 weeks of gestational age suffered from BPD.[2] BPD is a major cause of lethality and long-term morbidities, despite technological progress in neonatal intensive care medicine. Unfortunately, the mechanisms involved in BPD pathogenesis are still unclear. Therefore, it is particularly important to elucidate the pathogenic mechanisms of BPD.

According to their genomic localization in relation to nearby coding genes, lncRNAs are divided into intergenic, bidirectional, antisense, overlapping or intronic lncRNAs. lncRNAs are involved in many biological processes, such as chromatin remodelling, X-chromosome inactivation, imprinting, post-transcriptional regulation and embryonic stem cell pluripotency.[19–21] The expression profiles and roles of lncRNAs in BPD remain unclear, so we successfully established a hyperoxia-induced neonatal mouse BPD model and compared lncRNA expression profiles between BPD and normal groups. Mice born spontaneously at term

Table 3. Messenger RNAs implicated in bronchopulmonary dysplasia

Gene symbol	Accession number	RNA length	Chromosome	Log2 (O_2-treated/room air)
Sprr2a2	ENSMUST00000090871	722	chr3	−41·873
Cyp3a11	NM_007818	2053	chr5	−38·010
Apol11b	NM_001143686	2057	chr15	−32·571
Slc22a19	NM_144785	1984	chr19	−22·205
Ambp	NM_007443	1233	chr4	−20·950
Afp	NM_007423	2086	chr5	−14·558
Fabp1	NM_017399	492	chr6	−14·110
Zmat4	NM_177086	4206	chr8	−13·580
Aadac	NM_023383	1294	chr3	−13·190
Kng1	NM_023125	1950	chr16	−13·091
Fam19a4	NM_177233	2182	chr6	−11·652
Akr1c6	NM_030611	1359	chr13	−11·379
Cyp4a14	NM_007822	2503	chr4	−10·842
Lsp1	NM_001271508	2079	chr7	−10·759
Slitrk6	NM_175499	4243	chr14	−10·433
Gypa	NM_010369	1827	chr8	−10·209
Oxgr1	NM_001001490	3732	chr14	−9·668
Ahsg	ENSMUST00000023583	1474	chr16	−8·784
Pzp	NM_007376	4681	chr6	−8·743
Nusap1	NM_001042652	2861	chr2	−8·708
Bub1	NM_001113179	4337	chr2	−8·617
Acmsd	NM_001033041	2303	chr1	−8·557
Cenpf	NM_001081363	11130	chr1	−8·306
Alb	NM_009654	2043	chr5	−8·286
2810417H13Rik	NM_026515	2387	chr9	−8·251
Vsnl1	NM_012038	1951	chr12	−8·188
Dscc1	NM_183089	1327	chr15	−8·165
Nusap1	NM_133851	2960	chr2	−8·138
Bub1	NM_009772	4334	chr2	−8·114
Hist1h1a	NM_030609	747	chr13	−8·109
Pbk	NM_023209	1663	chr14	−7·981
Spc25	NM_025565	1212	chr2	−7·557
Ugt2b1	NM_152811	2560	chr5	−7·517
Lrr1	NM_001081406	1501	chr12	−7·484
Angptl7	NM_001039554	2062	chr4	−7·306
Olfr558	NM_147093	2923	chr7	−7·177
Mest	NM_001252292	2680	chr6	−7·098
Hist1h3c	NM_175653	480	chr13	−7·043
Ccne2	NM_009830	3023	chr4	−7·012
Veph1	NM_145820	6450	chr3	−7·004
I830012O16Rik	NM_001005858	2013	chr19	7·021
Trib3	NM_175093	2051	chr2	7·091
Cxcl17	NM_153576	760	chr7	7·162
Gdf15	NM_011819	1084	chr8	7·336
Ncan	NM_007789	7184	chr8	7·637
1700112E06Rik	NM_028275	911	chr14	7·739
Fbxw14	NM_015793	1497	chr9	8·132
Slc10a6	NM_029415	2124	chr5	8·212
Serpina3i	NM_001199940	2193	chr12	8·480
Gm12429	NM_001277167	4146	chr4	8·557
Smim18	NM_001206849	602	chr8	8·573
Cbln2	NM_172633	2201	chr18	8·848
Reg3g	NM_011260	774	chr6	9·237
2900011O08Rik	NM_144518	2355	chr16	9·512
Nhlh1	NM_010916	2506	chr1	9·964
Barhl2	NM_001005477	2329	chr5	10·144
Cdkn1a	NM_001111099	1936	chr17	10·540
Neurod1	NM_010894	2494	chr2	10·893
Saa2	NM_011314	610	chr7	12·185
Fezf1	NM_028462	2308	chr6	13·731
Cxcl2	NM_009140	1083	chr5	15·110
Ano3	NM_001128103	6026	chr2	16·999
Cxcl10	NM_021274	1120	chr5	17·446
Saa3	NM_011315	531	chr7	20·065
Neurod6	NM_009717	2154	chr6	21·213

(*Continues*)

Table 3. (Continued)

Gene symbol	Accession number	RNA length	Chromosome	Log2 (O_2-treated/room air)
Zbtb16	NM_001033324	5114	chr9	26·843
Npbwr1	NM_010342	3692	chr1	29·215
Cryge	NM_007777	662	chr1	43·650

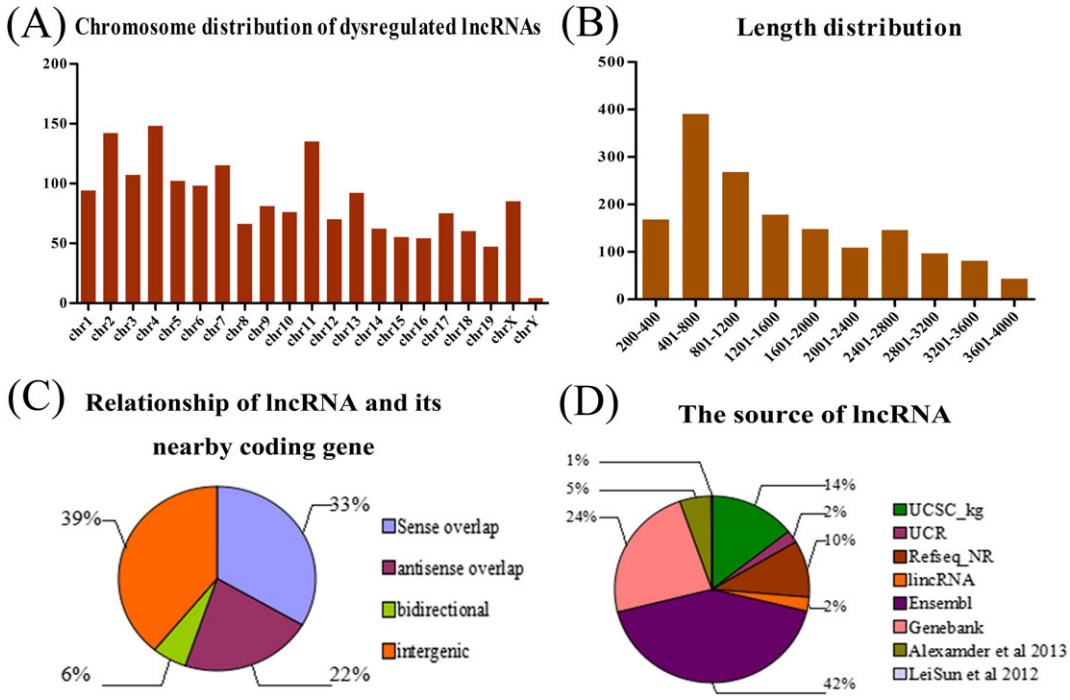

Figure 3. Expression signatures of dysregulated long non-coding RNAs (lncRNAs). (A) Chromosome locations of dysregulated lncRNAs. (B) Length distribution of dysregulated lncRNAs. (C) Percentage of different classifications of dysregulated lncRNAs. (D) Percentage of dysregulated lncRNAs identified from different databases.

reach the same lung developmental stage as extremely premature human neonates.[22,23] It has been shown that newborn mice exposed to high concentrations of ambient oxygen display morphological and pathological characteristics of BPD.[23,24] To a great extent, this murine model simulates BPD development among prematurely born human infants.

Using the third-generation high-throughput lncRNA microarray technology, we screened approximately 2000 aberrantly expressed (≥2-fold) lncRNAs in BPD lung tissues. We randomly selected and identified five upregulated lncRNAs and ten downregulated lncRNAs by qPCR. The results were consistent with microarray data. This approach demonstrated that a high oxygen concentration results in differential expression of lncRNAs and suggests that these lncRNAs may participate in the development of BPD. Currently, it is well known that lncRNA transcription usually regulates the expression of nearby protein-coding genes and targets distant activators or repressors to exert their biological function.[9,25] Therefore, we compared differentially expressed lncRNAs with differentially expressed mRNAs for target prediction.

Tenascin C is a transitional extracellular matrix protein that appears at the epithelial–mesenchymal interface during branching morphogenesis, and this expression pattern indicates that TNC plays an important role in promoting airway ramification.[26] Aberrant TNC expression in the lung is thought to modulate inflammatory cell influx.[27,28] TNC is minimally expressed in the adult lung but is highly induced following several forms of lung injury in both humans and mice.[29]

Our microarray and qPCR analyses confirmed that TNC mRNA expression was higher during the development of BPD than in controls. These findings are consistent with the results of Carey *et al.* who reported that a TNC deficiency alleviated TGF-β-mediated fibrosis following murine lung injury.[30] TGF-β initiates fibroblast proliferation and transformation to the myofibroblast phenotype and drives the pathological deposition of the collagen in the lung parenchyma by activating interstitial fibroblasts.[31] TGF-β also

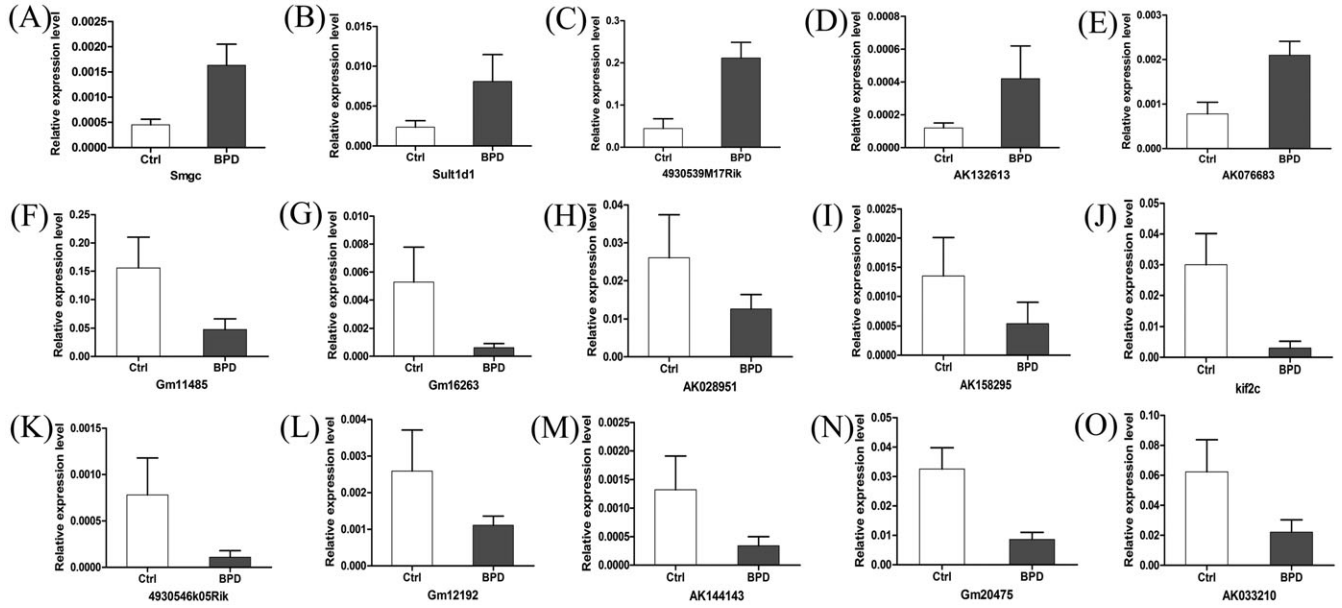

Figure 4. Relative expression of candidate long non-coding RNAs (lncRNAs) during the development of BPD validated by quantitative polymerase chain reaction. (A–E) Upregulated lncRNAs during the development of BPD. (F–O) Downregulated lncRNAs during the development of BPD. All $p < 0{\cdot}05$. BPD, bronchopulmonary dysplasia; Ctrl, control

plays an important role in early acute lung injury. For example, TGF-β promotes alveolar oedema formation and induces the expression of the transitional extracellular matrix found in early acute lung injury.[29,32] TGF-β activity in the lung is primarily mediated by the phosphorylation of the signalling molecules Smad-2 and Smad-3.[33] TNC is a ligand of

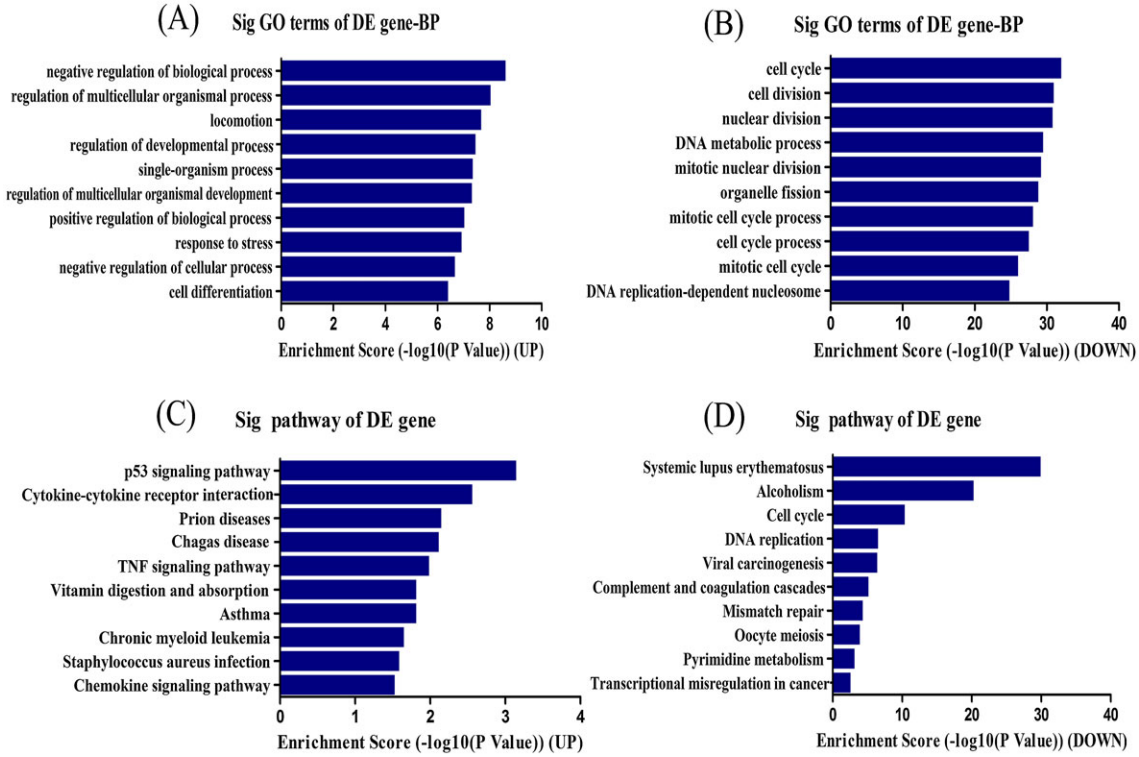

Figure 5. Gene ontology (GO) and pathway analyses of the differentially expressed long non-coding RNAs (lncRNAs). (A and B) Top ten GO terms for upregulated and downregulated lncRNAs. (C and D) Top ten pathways corresponding to the upregulated and downregulated lncRNAs

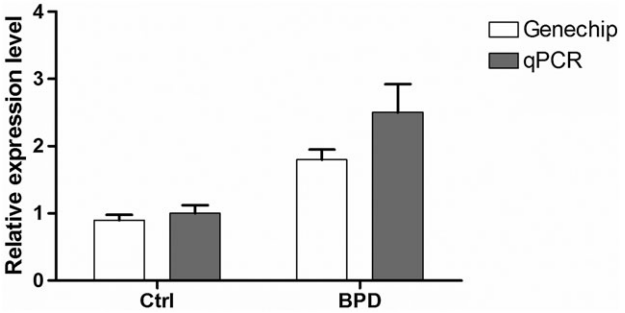

Figure 6. Tenascin C mRNA expression was higher during the development of bronchopulmonary dysplasia (BPD) than in controls (Ctrl) validated by quantitative polymerase chain reaction (qPCR) in eight pairs of lung tissue samples, and this result is consistent with GeneChip data

$\alpha v\beta 3$ integrin that may promote the progression of interstitial fibrosis by facilitating myofibroblast differentiation and proliferation through its interaction with $\alpha v\beta 3$ integrin.[34]

Moreover, TNC is known to restrain RhoA-mediated activation of the extracellular regulated kinase (Erk) pathway in fibroblasts.[35] Erk signalling opposes Smad-dependent TGF-β signalling in lung epithelial cell lines and could therefore potentially regulate epithelial–mesenchymal and mesenchymal–epithelial transitions.[36] Because TNC expression is highly restricted in adult tissues, the modulation of TNC function may allow for treatment approaches that are more specifically targeted to the lung than systemic treatment strategies that directly target TGF-β.[37] The downregulated expression of an lncRNA, AK033210, was negatively correlated with its nearby coding gene TNC. Given the important function of TNC in fibrosis, we speculate that AK033210 may participate in BPD development by regulating TNC expression. However, further studies are necessary to determine the molecular mechanisms and biological functions of AK033210 in BPD.

In conclusion, we screened differentially expressed lncRNAs in hyperoxia-induced BPD and found that 882 lncRNAs were upregulated and 887 lncRNAs were downregulated in BPD lungs compared with control lungs. To our knowledge, this study is the first to identify dysregulated lncRNAs associated with BPD development. Some of the candidate lncRNAs are involved in BPD development, but the exact biological functions, signalling pathways and molecular mechanisms of these lncRNAs need to be further investigated.

CONFLICT OF INTEREST

None declared.

ACKNOWLEDGEMENTS

This work was supported by grants from the Clinical Medicine Specialized Program of Jiangsu Province (BL2014063) and the Application Research and Scientific & Technological Project of Huai'an (HAS2014010).

REFERENCES

1. Northway WJ, Rosan RC, Porter DY. Pulmonary disease following respirator therapy of hyaline-membrane disease. Bronchopulmonary dysplasia. *N Engl J Med* 1967; **276**: 357–368.
2. Horbar JD, Carpenter JH, Badger GJ, *et al.* Mortality and neonatal morbidity among infants 501 to 1500 grams from 2000 to 2009. *Pediatrics* 2012; **129**: 1019–1026.
3. Baraldi E, Filippone M. Chronic lung disease after premature birth. *N Engl J Med* 2007; **357**: 1946–1955.
4. Manktelow BN, Draper ES, Annamalai S, Field D. Factors affecting the incidence of chronic lung disease of prematurity in 1987, 1992, and 1997. *Arch Dis Child Fetal Neonatal Ed* 2001; **85**: 33–35.
5. Kallapur SG, Jobe AH. Contribution of inflammation to lung injury and development. *Arch Dis Child Fetal Neonatal Ed* 2006; **91**: 132–135.
6. Hadchouel A, Delacourt C. Bronchopulmonary dysplasia and genetics. *Med Sci (Paris)* 2013; **29**: 821–823.
7. Szafranski P, Dharmadhikari AV, Brosens E, *et al.* Small noncoding differentially methylated copy-number variants, including lncRNA genes, cause a lethal lung developmental disorder. *Genome Res* 2013; **23**: 23–33.
8. Sauvageau M, Goff LA, Lodato S, *et al.* Multiple knockout mouse models reveal lincRNAs are required for life and brain development. *ELIFE* 2013; **2**: e1749.
9. Ponting CP, Oliver PL, Reik W. Evolution and functions of long noncoding RNAs. *Cell* 2009; **136**: 629–641.
10. Zeng Q, Wang Q, Chen X, *et al.* Analysis of lncRNAs expression in UVB-induced stress responses of melanocytes. *J Dermatol Sci* 2016; **81**: 53–60.
11. Huang S, Lu W, Ge D, *et al.* A new microRNA signal pathway regulated by long noncoding RNA TGFB2-OT1 in autophagy and inflammation of vascular endothelial cells. *Autophagy* 2015; **11**: 2172–83.
12. Lu W, Huang SY, Su L, Zhao BX, Miao JY. Long noncoding RNA LOC100129973 suppresses apoptosis by targeting miR-4707-5p and miR-4767 in vascular endothelial cells. *Sci Rep* 2016; **6**: 21620.
13. Yang Q, Xu E, Dai J, *et al.* A novel long noncoding RNA AK001796 acts as an oncogene and is involved in cell growth inhibition by resveratrol in lung cancer. *Toxicol Appl Pharmacol* 2015; **285**: 79–88.
14. Balasubramaniam V, Tang JR, Maxey A, Plopper CG, Abman SH. Mild hypoxia impairs alveolarization in the endothelial nitric oxide synthase-deficient mouse. *Am J Physiol Lung Cell Mol Physiol* 2003; **284**: 964–971.
15. Pfaffl MW. A new mathematical model for relative quantification in real-time RT-PCR. *Nucleic Acids Res* 2001; **29**: e45.
16. Gauldie J, Galt T, Bonniaud P, Robbins C, Kelly M, Warburton D. Transfer of the active form of transforming growth factor-beta 1 gene to newborn rat lung induces changes consistent with bronchopulmonary dysplasia. *Am J Pathol* 2003; **163**: 2575–2584.
17. Capoluongo E, Ameglio F, Zuppi C. Insulin-like growth factor-I and complications of prematurity: a focus on bronchopulmonary dysplasia. *Clin Chem Lab Med* 2008; **46**: 1061–1066.
18. Asikainen TM, Waleh NS, Schneider BK, Clyman RI, White CW. Enhancement of angiogenic effectors through hypoxia-inducible factor in preterm primate lung *in vivo*. *Am J Physiol Lung Cell Mol Physiol* 2006; **291**: 588–595.
19. Mercer TR, Dinger ME, Mattick JS. Long non-coding RNAs: insights into functions. *Nat Rev Genet* 2009; **10**: 155–159.
20. Kogo R, Shimamura T, Mimori K, *et al.* Long noncoding RNA HOTAIR regulates polycomb-dependent chromatin modification and is associated with poor prognosis in colorectal cancers. *Cancer Res* 2011; **71**: 6320–6326.
21. Wang KC, Chang HY. Molecular mechanisms of long noncoding RNAs. *Mol Cell* 2011; **43**: 904–914.
22. Maeda Y, Dave V, Whitsett JA. Transcriptional control of lung morphogenesis. *Physiol Rev* 2007; **87**: 219–244.
23. Dong J, Kislinger T, Jurisica I, Wigle DA. Lung cancer: developmental networks gone awry? *Cancer Biol Ther* 2009; **8**: 312–318.
24. Alejandre-Alcazar MA, Kwapiszewska G, Reiss I, *et al.* Hyperoxia modulates TGF-beta/BMP signaling in a mouse model of bronchopulmonary dysplasia. *Am J Physiol Lung Cell Mol Physiol* 2007; **292**: 537–549.

25. Mattick JS, Gagen MJ. The evolution of controlled multitasked gene networks: the role of introns and other noncoding RNAs in the development of complex organisms. *Mol Biol Evol* 2001; **18**: 1611–1630.
26. Kaarteenaho-Wiik R, Kinnula V, Herva R, Paakko P, Pollanen R, Soini Y. Distribution and mRNA expression of tenascin-C in developing human lung. *Am J Respir Cell Mol Biol* 2001; **25**: 341–346.
27. Amin K, Ludviksdottir D, Janson C, *et al.* Inflammation and structural changes in the airways of patients with atopic and nonatopic asthma. BHR group. *Am J Respir Crit Care Med* 2000; **162**: 2295–2301.
28. Zuo F, Kaminski N, Eugui E, *et al.* Gene expression analysis reveals matrilysin as a key regulator of pulmonary fibrosis in mice and humans. *Proc Natl Acad Sci U S A* 2002; **99**: 6292–6297.
29. Kaminski N, Allard JD, Pittet JF, *et al.* Global analysis of gene expression in pulmonary fibrosis reveals distinct programs regulating lung inflammation and fibrosis. *Proc Natl Acad Sci U S A* 2000; **97**: 1778–1783.
30. Carey WA, Taylor GD, Dean WB, Bristow JD. Tenascin-C deficiency attenuates TGF-β-mediated fibrosis following murine lung injury. *Am J Physiol Lung Cell Mol Physiol* 2010; **299**: 785–793.
31. Datto M, Wang XF. Ubiquitin-mediated degradation a mechanism for fine-tuning TGF-beta signaling. *Cell* 2005; **121**: 2–4.
32. Frank J, Roux J, Kawakatsu H, *et al.* Transforming growth factor-beta1 decreases expression of the epithelial sodium channel alphaENaC and alveolar epithelial vectorial sodium and fluid transport via an ERK1/2-dependent mechanism. *J Biol Chem* 2003; **278**: 43939–43950.
33. Evans RA, Tian YC, Steadman R, Phillips AO. TGF-beta1-mediated fibroblast-myofibroblast terminal differentiation—the role of Smad proteins. *Exp Cell Res* 2003; **282**: 90–100.
34. Yokoyama K, Erickson HP, Ikeda Y, Takada Y. Identification of amino acid sequences in fibrinogen gamma-chain and tenascin C-terminal domains critical for binding to integrin alpha vbeta 3. *J Biol Chem* 2000; **275**: 16891–16898.
35. Williams SA, Schwarzbauer JE. A shared mechanism of adhesion modulation for tenascin-C and fibulin-1. *Mol Biol Cell* 2009; **20**: 1141–1149.
36. Ramos C, Becerril C, Montano M, *et al.* FGF-1 reverts epithelial-mesenchymal transition induced by TGF-{beta}1 through MAPK/ERK kinase pathway. *Am J Physiol Lung Cell Mol Physiol* 2010; **299**: 222–231.
37. Fukasawa H, Yamamoto T, Suzuki H, *et al.* Treatment with anti-TGF-beta antibody ameliorates chronic progressive nephritis by inhibiting Smad/TGF-beta signaling. *Kidney Int* 2004; **65**: 63–74.